

Metallocene-catalyzed polymerization of ethylene in the presence of graphite. II. Structure and electrical properties of the composites

Mirosław Pluta^a, Michaël Alexandre^{b, 1}, Silvia Blacher^c, Philippe Dubois^{b, 1} and Robert Jérôme^b

^a Center of Molecular and Macromolecular Studies, Polish Academy of Sciences, Sienkiewicza 112, 90-363 Lodz, Poland

^b Center for Education and Research on Macromolecules (CERM), University of Liège, Sart-Tilman, B6, 4000 Liège, Belgium

^c Laboratoire de Génie Civil, University of Liège, Sart-Tilman, B6, 4000 Liège, Belgium

Abstract

Structure and electrical properties of conducting polyethylene/graphite composites have been studied in relation to the preparation method, i.e. (i) the polymerization-filling technique (PFT), in which the polyolefinic chains are growing from the graphite surface, (ii) the slurry polymerization of ethylene in the presence of untreated graphite, and (iii) the mechanical blending of preformed polyethylene and graphite. The extent of the filler dispersion depends on the method used for the composite preparation. Moreover, the graphite particles can be oriented by the molding of the samples used for the measurement of the electrical properties. This orientation is as pronounced as the melt viscosity of polyethylene is low, this characteristic feature changing with the preparation method. These structural details have consequences on the electrophysical properties and the percolation threshold. Finally, the thermal dependence of the electrical resistivity has been studied.

Keywords: Composite; Polymerization-filling technique; Mechanical blending

1. Introduction

The range of properties of the organic polymers can be increased by various methods, including modification by inorganic fillers. Loaded by an electrically conducting filler, an insulating polymer can be endowed with electrical conductivity and find widespread applications, e.g. for antistatic protection, electromagnetic radiation shielding, prevention of crown discharge in high voltage cables, as low-temperature heaters, transducers, etc. [1].

Polyethylene is a matrix of choice for this type of applications, because of high insulating properties combined with high ductility and good processability. In addition to the direct melt blending of the preformed constitutive components, polyethylene composites can be prepared by the so-called polymerization-filling technique (PFT) [2-5]. In this case, ethylene is polymerized from the filler surface onto which the organometallic catalyst is anchored. The filler is more efficiently deagglomerated and dispersed, which results in improved mechanical properties with respect to the classical melt blending [6-8].

In this work, new conducting composites of high density polyethylene and graphite have been prepared by PFT with a methylalumoxane/metallocene complex as catalyst. For the sake of comparison, ethylene has also been polymerized with the same catalyst not previously bound to the graphite particles. Finally, composites with similar compositions have been prepared by mechanical blending of melted high-density polyethylene and neat graphite particles. For each of the three preparation methods, the dependence of the electrical properties on the composite morphology has been studied. The morphology has been analyzed by scanning electron microscopy (SEM) and quantified by image analysis. The sample characterization has been completed by DSC and thermogravimetric (TGA) analyses. The electrical properties have been measured in relation to the filler content and tentatively related to the filler dispersion and orientation.

2. Experimental

2.1. Preparation of composites

Synthetic graphite EP1002 (mean particle size: 2 μm , specific surface area: 16.9 m^2/g) from N.V. Contimet S.A. (Brussels) was used as a filler. The particles were flake-like shaped with an aspect ratio of ca. 4.

Three sets of polyethylene/graphite composites with various filler contents were prepared by three methods. (i) PFT in which ethylene was polymerized from the graphite surface, onto which a methylalumoxane/titanocene complex was previously anchored. Experimental details were published elsewhere [9]. Composites prepared by PFT are referred to as TGC (Treated Graphite Composites). (ii) polymerization of ethylene in the presence of non-treated graphite particles by the same methylalumoxane/metallocene complex dissolved in the reaction medium [9]. These composites are designated as NGC (Non-treated Graphite Composites). (iii) mechanical blending of commercially available high density polyethylene (DOW HDPE, $MW=1 \text{ g}/10 \text{ min}$) with non-treated graphite particles. MBC is the code used to identify these composites (Melt Blend Composites). Blending was performed with a two-roll mill at 195°C for 7 min. For graphite contents higher than 50 wt%, the filler was first hot-sandwiched into polyethylene foils, before being processed with the two-roll mill. All the samples (TGC, NGC and MBC) were compression molded as 1.5 mm thick plates at 195°C for 6 min and then quenched in the mold.

2.2. Characterization of composites

The graphite content of the composites was determined by TGA under air, with a DuPont 51 thermogravimetric analyzer at a heating rate of 20°C/min. It was calculated from the weight loss at 600°C, the weight of the solid residue (graphite) being constant then.

Thermal analysis was carried out with a DuPont 910 differential scanning calorimeter for compression molded samples, previously heated at 200°C and then slowly cooled down to room temperature. The temperature range from -150 to 200°C was scanned under nitrogen, at a heating rate of 10°C/min. The degree of crystallinity, X_c , was calculated from the experimental melting heat (ΔH_m , in J/g PE) and the melting enthalpy of 100% crystalline PE [10], i.e. $2.93 \times 10^{-5} \text{ J/kg}$. The melting temperature (T_m) was recorded at the maximum of the melting endotherm.

SEM was performed with a JEOL JSM-840A Scanning Microscope with gold-palladium metallized samples.

The image treatment and the image statistical analysis were carried out with a Sun Spark 30 computer and the 'Visilog' software from NOESIS. SEM micrographs were digitised in 1024×768 pixels with 256 gray levels. Electrical properties were measured with a Keithley 487 Picoammeter along the longer length (sample size: $20 \times 15 \times 1.5 \text{ mm}^3$). Silver paint was used to contact the sample surface and the silver electrodes. A two-point method was used for the samples filled with less than 40 wt% graphite, and a four-point method was used in case of graphite content exceeding 40 wt% in order to avoid any contribution of the contact resistance. Resistance was calculated from the slope of the current-voltage dependence. Temperature dependence of resistivity was recorded at a heating rate of 2°C/min. Resistivity data were expressed as relative values with respect to the reference measured at 20°C.

3. Results and discussion

The samples studied in this paper are listed in Table 1, together with the graphite content which lies in the ca. 10–75 wt% range.

Table 1. Composition of graphite/polyethylene composites prepared by three different methods

Treated graphite composites (TGC)		Non-treated graphite composites(NGC)		Melt blend composites (MBC)	
Composite code	Graphite content (wt%)	Composite code	Graphite content (wt%)	Composite code	Graphite content (wt%)
TGC1	8.1	NGC1	12.4	MBC1	5.5
TGC2	16.5	NGC2	15.6	MBC2	8.3
TGC3	22.1	NGC3	23.7	MBC3	12.8
TGC4	32.1	NGC4	26.4	MBC4	18.1
TGC5	38.0	NGC5	35.1	MBC5	20.8
TGC6	39.5	NGC6	49.4	MBC6	27.3
TGC7	43.1	NGC7	57.2	MBC7	38.8
TGC8	58.0	NGC8	82.9	MBC8	50.0
TGC9	70.0			MBC9	71.0

3.1. DSC analysis

DSC analysis of the TGC, NGC and MBC composites shows differences in the melting behavior in relation to the preparation method and the graphite content. The thermal analysis of the TGC and NGC samples was reported in a previous paper [9]. Fig. 1a,b illustrate typical DSC thermograms for NGC and TGC samples of two different graphite loadings (ca. 20 wt% in Fig. 1a, and 50 wt% in Fig. 1b). At low graphite loading (i.e. NGC 2: 15.6 wt% graphite and TGC 3: 20.0 wt% graphite; Fig. 1a) the thermograms are comparable and featured by a low temperature 'tail' and a main melting peak at 141.5°C for NGC2 and 141°C for TGC3. The heat of melting is, however, much lower for the composite prepared by the PFT (TGC3: 205 J/g PE) than for the composite prepared by polymerization of ethylene in the presence of untreated graphite (NGC2: 223 J/g PE). This difference in the crystalline structure of PE (crystallite size and size distribution, crystallization defects,...) is the consequence of modifications in the graphite dispersion and the particle-matrix interaction triggered by the preparation method used. At higher filler loading (Fig. 1b), the differences between the two series of composites are magnified. The low temperature tail of the endotherms is more pronounced, particularly for the TGC sample, consistently with a larger population of less ordered and thus less thermally stable crystallites at the vicinity of the chemically modified surface of graphite [9]. Moreover, the main melting peak is sharper and the melting temperature is lower, which reflects an adversary effect of the high filler content on the crystallite size and perfection. Finally, the lower heat of melting for the TGC sample ($\Delta H_m=194.0$ J/gPE) indicates a strong decrease in the PE crystallinity, which is even more pronounced ($\Delta H_m=180$ J/gPE) at a still higher filler loading (70 wt%).

The DSC thermograms have also been recorded for the MBC samples, and the calorimetric data are collected in Table 2. For this type of composites, the graphite content has a limited effect on the melting behavior. The values of X_c and T_m are essentially comparable for all the composites prepared by melt blending, which is not surprising, because these composites contain the same HDPE and no interaction should occur at the interface between the polymer and the filler.

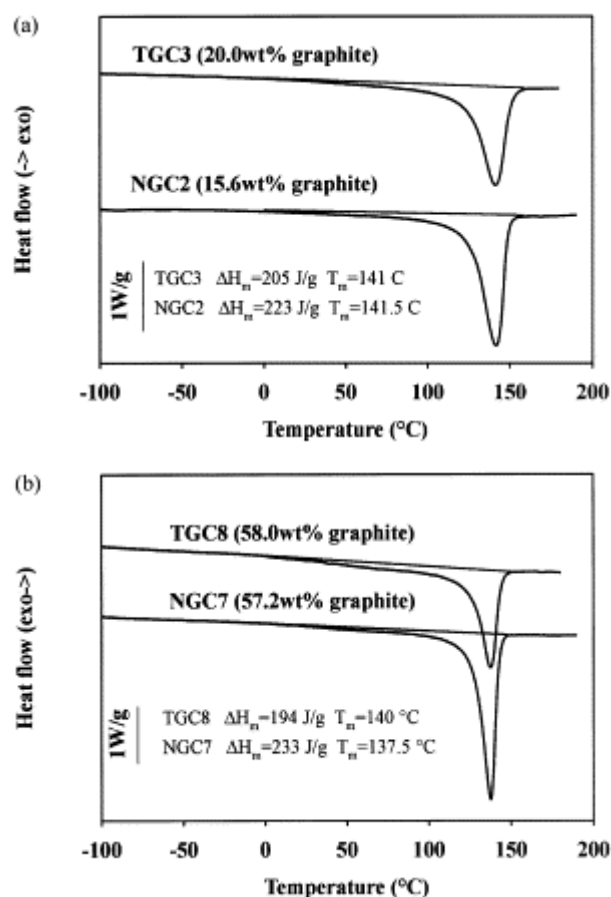


Fig. 1. DSC thermograms, heat of melting (ΔH_m) and melting temperature for NGC and TGC composites containing: (a) ca. 20 wt% of graphite, (b) ca. 60 wt% of graphite.

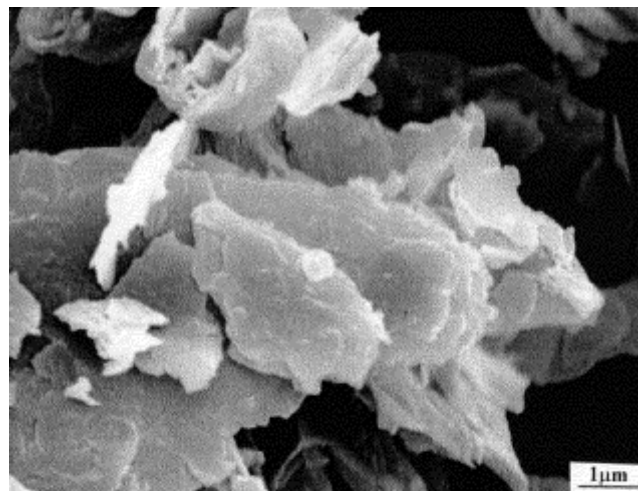
Table 2. Degree of crystallinity (X_c) and melting temperature (T_m) for the melt blended composites (n.d.=not determined)

Composite code	Graphite content (wt%)	X_c (%)	T_m (°C)
MBC1	5.5	71.3	140.0
MBC2	8.3	71.0	140.9
MBC3	12.8	74.3	138.8
MBC4	18.1	71.8	139.9
MBC5	20.8	73.6	139.4
MBC6	27.3	71.9	139.8
MBC7	38.8	71.9	140.5
MBC8	50.0	73.6	138.7
MBC9	71.0	n.d.	n.d.

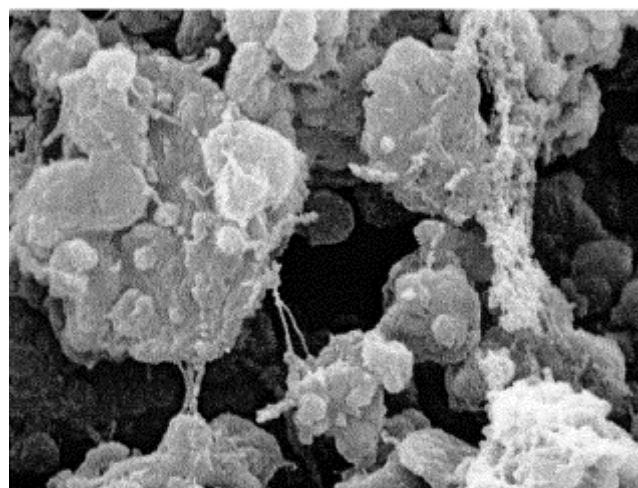
3.2. Scanning electron microscopy

Graphite and the as-recovered TGC and NGC samples (i.e. after synthesis and drying) were observed by SEM in order to figure out how the polymer chains have grown in the presence of treated and non-treated graphite particles, respectively. The graphite particles are flake-like shaped, and they consist of stacks of thin plates (Fig. 2a). A mean particle size of ca. 2 μm and an aspect ratio of ca. 4 have been extracted from the SEM images. Fig. 2b shows a typical micrograph for the as-recovered TGC6 sample (60.5 wt% PE). This micrograph shows that the pretreated filler particles are covered by a polyethylene layer, onto which polymer microglobules are observed. Some filler particles are mutually connected by polymer fibers. This structural feature was also reported for composites prepared by PFT, e.g. kaolin-filled polyethylene [11]. It is a direct consequence of the growth of the polymer chains from the treated filler surface. The structure of composites containing untreated graphite is exemplified by the NGC2 sample (84.4 wt% PE) in Fig. 2c. The morphology is quite different from

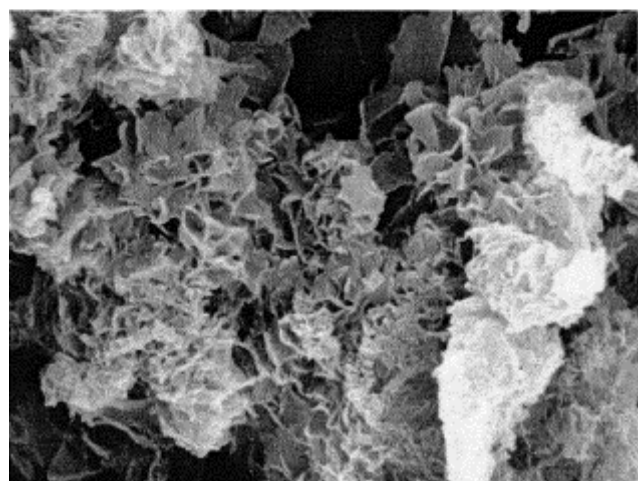
TGC6 (Fig. 2b), but very close to that one commonly observed for polyethylene formed with non-supported catalysts.



(a)



(b)



(c)

Fig. 2. SEM micrographs for: (a) neat graphite powder; (b) powdery TGC6 (39.5 wt% of graphite); (c) powdery NGC2 (15.6 wt% of graphite).

Cryofractured surfaces of compression molded composites were also observed for samples prepared by each of the three methods. SEM micrographs of selected composites, i.e. TGC8 (58 wt% graphite), NGC6 (49.4 wt% graphite) and MBC8 (50 wt% PE) are shown in Fig. 3b–d. Fig. 3a schematizes the relative orientation of the micrographs with respect to the direction of the compression molding. The most ‘homogeneous’ dispersion of the graphite particles within polyethylene is observed for the TGC sample. In contrast, the SEM micrographs of the NGC (Fig. 3c) and MBC samples (Fig. 3d) show some platelets oriented parallel to the sample surface (molding plane). Moreover, the filler dispersion is coarser in the MBC samples compared to composites prepared by direct synthesis of PE in the presence of graphite (TGC). This observation confirms that the filler particles are more efficiently deagglomerated when polymerization is carried out ‘in-situ’ (NGCs, TGCs).

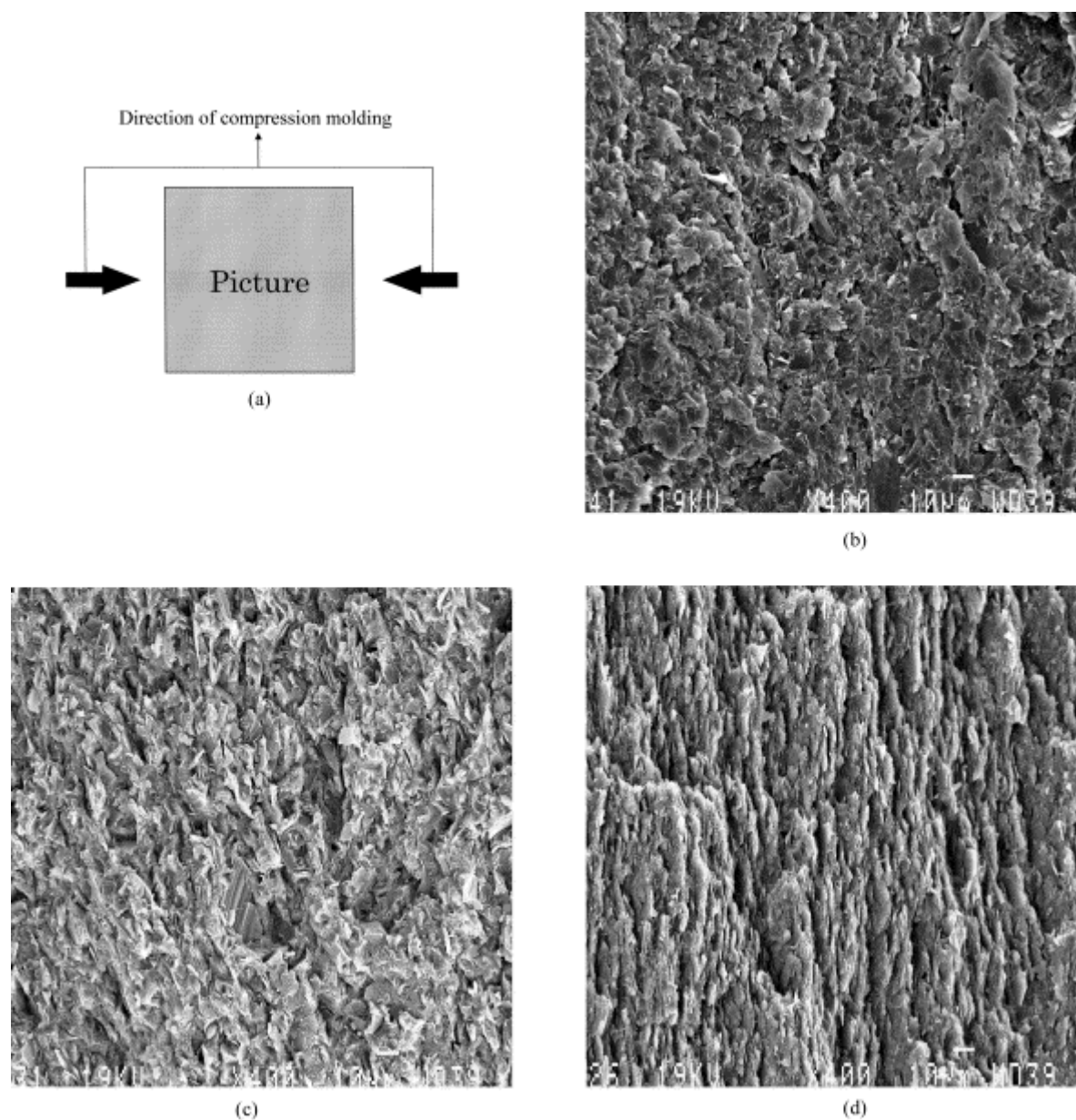


Fig. 3. (a) Orientation of the micrographs with respect to the molding pressure; SEM micrographs of cryofractured composites: (b) TGC8 (58.0 wt% of graphite); (c) NGC6 (49.4 wt% of graphite); (d) MBC8 (50.0 wt% of graphite).

3.3. Image analysis

In order to quantify the degree of orientation of the graphite particles in the cryofractured samples, the following treatment was performed:

Enhancement of local discontinuities or edges of the images by gradient techniques [12]. The most emphasised features are basically the boundaries of the surface fracture.

Thresholding of the local image gradient, with the purpose to maintain only sharp enough gray level transitions as edge points.

Analysis of the directional structure of the edges of the binary image by computation of the rose of directions. The number of edges oriented in one direction between 0 and 180° (i.e. the horizontal direction) is actually counted.

Fig. 4a–c shows the superimposition of the threshold image on the original one for the three types of samples (TGC, NGC, MBC). A visual comparison of Fig. 3 and Fig. 4 confirms that most boundaries of the surface fracture are emphasized by the image treatment. Fig. 5a–c shows the histograms of the number of segments on the edges for a series of angle between 0 and 180° (steps of 30°). These graphs show that most contours are oriented at 90° (parallel to the molding plane) for the MBC8 sample and that this preferential orientation is less marked in NCG6 and almost lost in TGC8 (no preferential orientation of the filler).

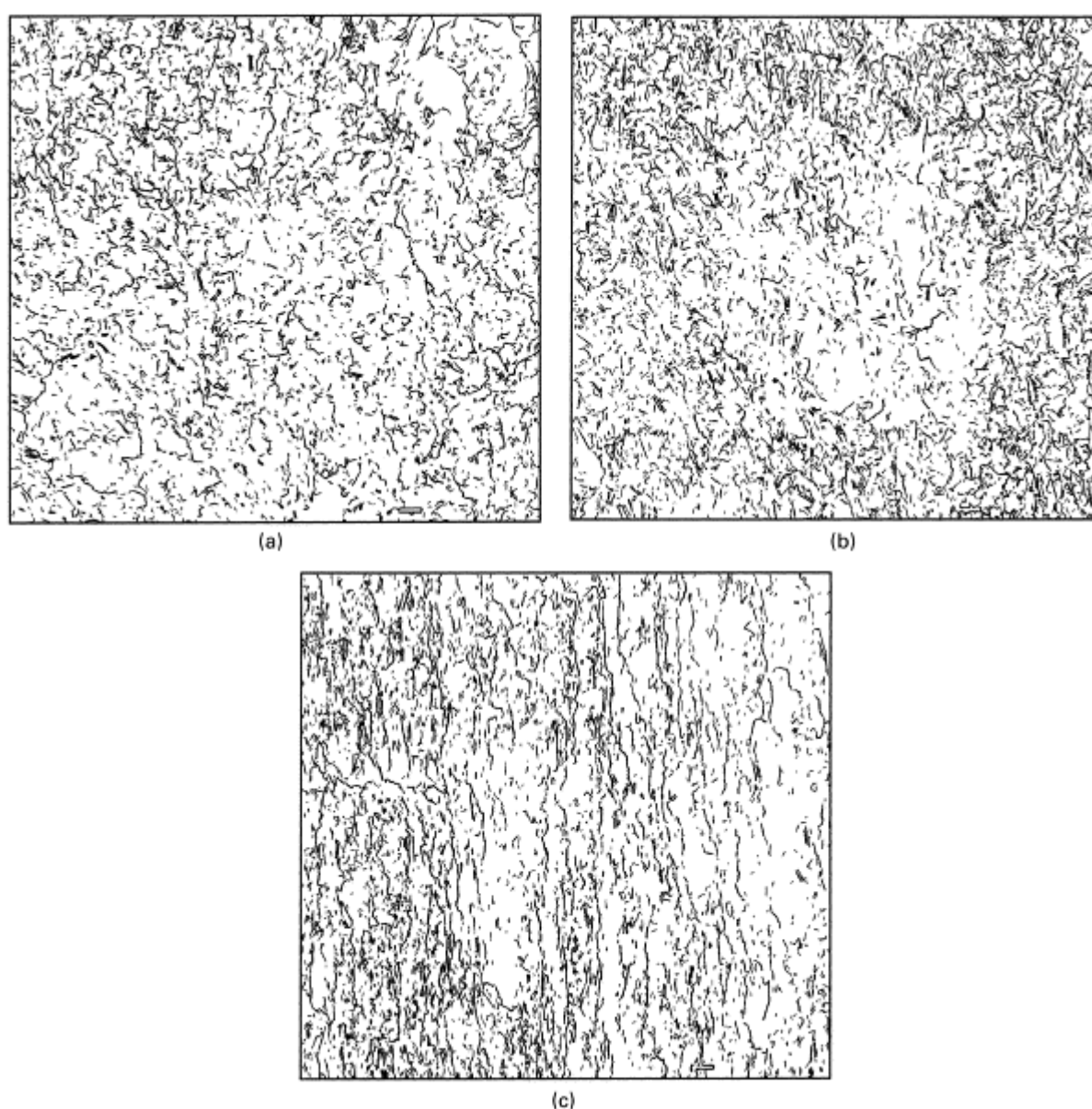


Fig. 4. Computerized images of SEM micrographs for: (a) TGC8 (from Fig. 3b); (b) NGC6 (from Fig. 3c); (c) MBC8 (from Fig. 3d).

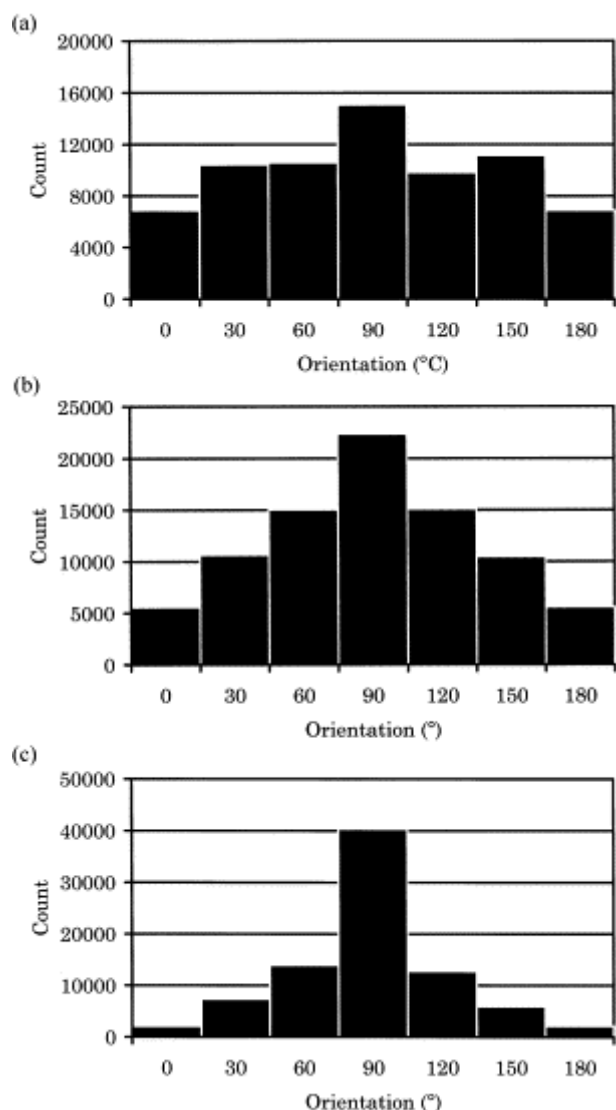


Fig. 5. Graphite orientation extracted from the computerized micrographs by image analysis: (a) TGC8 (from Fig. 4a); (b) NGC6 (from Fig. 4b); (c) MBC8 (from Fig. 4c).

The origin for differences in the filler orientation may be found, at least partly, in the melt viscosity, η , of the composites prepared by the three different methods. Accordingly, the melt viscosity at comparable composition, should be classified as $\eta(\text{NGC}) \cong \eta(\text{MBC}) < \eta(\text{TGC})$. The highest viscosity of the TGC sample is quite consistent with the observation that (ultra) high molecular weight polyethylene is formed in the PFT [1]. It must be noted that the filler orientation is expected to depend not only on the inherent viscosity of the polymer but also on other phenomena, such as the filler deagglomeration and interactions with the polymer as for other filled polymers [5].

3.4. Electrical properties

The dependence of the specific resistivity (ρ) of the composites on the graphite content is shown in Fig. 6. Eq. (1) was used to calculate the graphite content in vol% from the weight composition, the graphite density ($d_{\text{graphite}}=2.18$, as measured by pycnometry in decaline) and the HDPE density approximated to 0.96.

$$\text{vol\%}(\text{graphite}) = \frac{100}{\left[\left(\frac{d(\text{graphite})}{d(\text{matrix})} \frac{\text{wt\%}(\text{matrix})}{\text{wt\%}(\text{graphite})} \right) + 1 \right]}$$

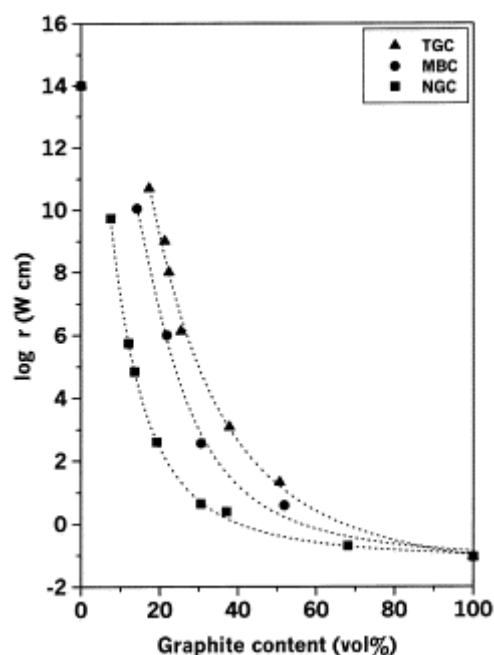


Fig. 6. Specific resistivity vs graphite content (vol%), for composites prepared by different methods: TGC (triangle), NGC (square) MBC (circle).

Whatever the preparation method, the resistivity of the composites expectedly decreases with increasing graphite content. However, the drop in resistivity is observed at filler loading, which is directly related to the filling technique. At a constant graphite content, the resistivity of the NGCs is lower than the one of the MBCs, which in turn is lower than for the TGCs. These differences may be as large as two orders of magnitude at a graphite content of 35 vol%. The percolation threshold, c_t , is usually defined as the filler content at which an infinite cluster of filler particles is formed, thus at which a sharp drop in resistivity occurs, in case of conductive particles. The percolation theory predicts that $c_t=18$ vol% for conducting particles of a spherical shape [13]. According to Fig. 6, the percolation threshold changes in agreement with the $c_t(\text{NGC}) < c_t(\text{MBC}) < c_t(\text{TGC})$ sequence. Although, it is difficult to determine c_t accurately, it appears that the threshold for the MBC series is close to the theoretical value, whereas it is lower for the NGC samples and higher for the TGCs. Discrepancy from the theoretical predictions was also reported for other conducting systems [14-16]. It can be explained by the interplay of various factors, such as type [17], shape [18], structuring ability [19], and surface properties of the filler, chemical and physical properties of the polymer matrix [20], and preparation method or processing conditions [21], etc. The electrical data reported for the composites under consideration are in qualitative agreement with the internal structure observed by SEM and the image analysis of the micrographs. Indeed, the higher resistivity of the TGC samples is consistent with the fine and homogeneous dispersion of the filler and the absence of preferential orientation.

The percolation threshold is significantly lower in the NGC samples because of some preferential orientation of the filler particles in the probing direction (parallel to the sample surface). This partial alignment of graphite is favorable to the earlier formation of conducting pathways. Moreover, contact of graphite with methylalumoxane and trimethyl-aluminum during the synthesis of the NGC composites can also contribute to a higher degree of dispersion of the filler, because the reaction of the surface hydroxyl groups prevents aggregation from occurring by hydrogen bonding [8]. As a result, the probability that conducting pathways are formed is increased. The intermediate resistivity of the MBC samples (Fig. 6) is primarily related to the gross dispersion of the filler particles. The mechanical blending is not efficient enough to deaggregate graphite stacks, which are however preferentially oriented in the direction of the resistivity measurement. The predominance of the former effect explains that contacts between the conductive particles are only possible at high enough filler content.

The temperature dependence of the resistivity has also been studied. Fig. 7 shows the relative change in resistivity with temperature (T), $\rho(T)/\rho(20)$ for the NGC4 sample, 20°C being selected as a reference. Similarly, the relative heat of melting, $\Delta H_m(T)/\Delta H_m$, has been plotted in the same figure. $\Delta H_m(T)$ and ΔH_m were extracted from the integration of the DSC endotherm area in the temperature interval from 20°C to T ($\Delta H_m(T)$) and from 20 to 190°C (total melting enthalpy, ΔH_m), respectively. It is clear from Fig. 7 that the resistivity directly

depends on the melting of the polyethylene matrix. A sharp rise in resistivity is observed above 100°C, i.e. as soon as the polymer starts to melt. Two phenomena contribute to this effect: (i) upon heating, the polymer matrix is expanded, and the average distance between the graphite particles is increased, (ii) the melting of the polymer matrix weakens or disrupts some conducting pathways. At a given temperature, the magnitude of the resistivity change, $\Delta\rho = \rho(T)/\rho(20)$, expectedly depends on the filler content. This effect is illustrated in Fig. 8 for the NGC samples. The same type of dependence was observed by Galashina et al. for polypropylene/graphite composites [16]. For $\Delta T \approx 100^\circ\text{C}$, an eight-fold increase in $\Delta\rho$ is reported for the NGC4 sample filled with 26.4 wt% graphite. At the higher graphite content (57.2 wt%), the jump in $\Delta\rho$ is small and it goes unobserved for the NGC8 composite that contains 82.9 wt% filler. Finally, the magnitude of $\Delta\rho$ depends on the method used for the composite preparation. For instance, $\Delta\rho$ has been measured for composites filled with a comparable graphite content (ca. 55 wt%: TGC8, NGC7 and MBC8). $\Delta\rho$ at $\Delta T = 100^\circ\text{C}$ is equal to 1.6, 3.7 and 2.2, respectively, which leads to the following ranking: $\Delta\rho(\text{NGC}) > \Delta\rho(\text{MBC}) > \Delta\rho(\text{TGC})$. Interestingly enough, the sequence in $\Delta\rho$ is the same as the melting enthalpy sequence: $\Delta H_m(\text{NGC}) > \Delta H_m(\text{MBC}) > \Delta H_m(\text{TGC})$, which confirms the relationship established between the composite morphology and the electrical properties at elevated temperature (Fig. 7). From this observation, one can anticipate that the composites prepared by PFT (TGC type) should display a higher stability and/or reproducibility of the electrophysical properties during cyclic changes of extrinsic conditions, such as mechanical deformation and temperature variation.

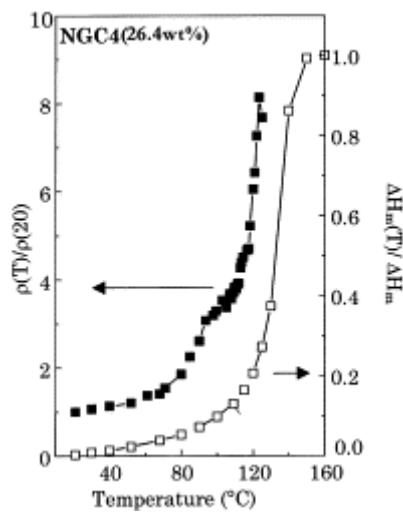


Fig. 7. Temperature dependence of the relative resistivity ($\Delta\rho = \rho(T)/\rho(20)$) and the relative melting enthalpy ($\Delta H_m(T)/\Delta H_m$) of the NGC4 sample.

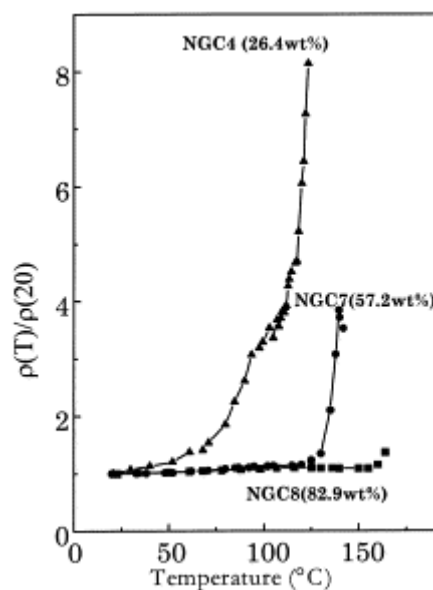


Fig. 8. Temperature dependence of the relative resistivity ($\Delta\rho=\rho(T)/\rho(20)$) for NGC samples with different graphite contents.

4. Conclusions

The electrical conductivity of polyethylene/ graphite composites can be tuned by changing the preparation method. At a constant filler content, this property increases from TGCs, through MBCs to NGCs. This evolution is related to modifications in the composite morphology that have direct influence on the percolation threshold.

Indeed, the homogeneous dispersion of deagglomerated graphite particles observed for NGCs, together with the low viscosity of the PE matrix, endows the filler with some preferential orientation which accounts for a low percolation threshold. This characteristic feature is increased in the case of MBCs, because the melt processing is unable to deagglomerate efficiently the graphite particles, which however show a pronounced orientation in the sample. When the composites are prepared by PFT, the graphite particles are deagglomerated in a highly viscous PE matrix, which prevents them from being oriented, and they are coated by the polymer deposited on their surface. As a result, the percolation threshold is considerably increased. The PFT has clearly a decisive role on the composite morphology and, accordingly, on the electrical properties. This technique is actually promising for applications in which durability and reproducibility of the electrophysical properties are required in spite of cyclic changes of external conditions, such as temperature variation and mechanical deformation.

Acknowledgements

M.A., Ph.D. and R.J. are indebted to the 'Services Fédéraux des Affaires Scientifiques, Techniques et Culturelles' for general support to CERM in the frame of the 'Pôles d'Attraction Interuniversitaires: Supramolecular Catalysis and Supramolecular Chemistry- PAI(4-11)'.

CERM. is also grateful to DOW Europe (Terneuzen, The Netherlands) for financial support and to Dr M. Garcia Marti for fruitful scientific discussions.

M.P. thanks the 'Belgium-Poland Scientific and Technological Cooperation' for a grant to visit CERM in Liège.

References

- [1] Gul' VE. Structure and properties of conducting polymer composites. 1st ed. Utrecht: VCR, 1996.
- [2] Enikolopian NS. USSR Pat 1976, 763,379
- [3] Howard EG. US Pat 1980, 4,187,210
- [4] Howard EG, Glazar BL, Collette JW. High performance plastics. Natl Tech Conf Soc Plast Eng (Prepr) 1976;36 Cleveland.
- [5] Dubois P, Alexandre M, Hindryckx F, Jérôme R. J Macromol Sci: Rev Macromol Chem Phys 1998;C38:511.
- [6] Howard EG, Lipscomb RD, MacDonald RN, Glazard BL, Tullock CW, Collette JW. Ind Engng Chem Prod Res Dev 1981;20:421.
- [7] Enikolopian NS, Fridman AA, Popov WL, Stalnowa IO, Briekenstein AA, Rudakov WM, Gherasina NP, Tchalykh AE. J Appl Polym Sci 1986;32:6107.
- [8] Hindryckx F, Dubois P, Jérôme R, Teyssié P, Garcia-Marti M. J Appl Polym Sci 1997;64:439.
- [9] Alexandre M, Pluta M, Dubois P, Jérôme R. Macromol Chem Phys. Accepted for publication.
- [10] Flory PJ, Vrij J. J Am Chem Soc 1963;85:3548.
- [11] Hindryckx F, Dubois P, Jérôme R, Teyssié P, Garcia-Marti M. J Appl Polym Sci 1997;64:423.
- [12] Coster M, Chermant JL. Précis d'analyse d'images. 1st ed. Paris: Presses du C.N.R.S., 1989.
- [13] Kirkpatrick S. Rev Mod Phys 1973;45:574.
- [14] Godovski DY, Sukharev VY, Volkov AV, Moskvina MA. Russ J Phys Chem 1993;67:1452.
- [15] Kotosonov AS, Kuvshinnikov SV, Tchmutin IA, Ponomarenko AT, Shevchenko VG, Enikolopyan NS. Vysokomol Soedin 1991;33:1746.
- [16] Galashina NM, Nedorezova PM, Shevchenko VG, Tsvtkova VI, Klyamkina AN, Chmutin IA, Ponomarenko AT, D'yachkovskii FS. Polym Sci USSR 1993;35:1089.
- [17] Giziano LE, Lupo G, Nicolais I, Nobile R, Tucci V. L'Energia Elet- trica 1985;3:125.
- [18] Carmona F, Amarti AE. Phys Rev B: Condens Matter 1987;35:3284.
- [19] Gul' VE, ShenFIT LZ. Elektroprovodyashchie polimernyye kompo-zitsii (Electroconductive polymer compositions). 1st ed. Moscow: Khimiya, 1984.
- [20] Wessling B. Synth Met 1973;40:1057.
- [21] Galashina NM, Nedorezova PM, Popov VL, Salamatina OB, Kish L, Nad' L, Ponomarenko AT, Shevchenko VG, Raspopov LN, Eniko- lopyan NS. Abstracts of XII Vses. Soveshch. po Organicheskim Polu-provodnikam (XIII All-Union Conf. on Organic Semiconductors), Moscow, 1984. p. 102.